Styrene thermal decomposition under shock tube pyrolysis conditions: an experimental and kinetic modeling study

HAMADI Alaa, CANO ARDILA Fabian-Esneider, SAID Abid, CHAUMEIX Nabiha, COMANDINI Andrea
ICARE-CNRS
Orleans, Loiret, France

Abstract

The goal of this paper is to present new experimental data on styrene pyrolysis using a single pulse shock tube and better understand the associated generation of polycyclic aromatic hydrocarbons (PAHs) from the parent fuel. Experiments are carried out at a residence time of 4 ms, a pressure of 20 bar, and temperatures ranging from 1160 to 1730 K. The styrene sub-mechanism is updated into our on-going PAH formation kinetic model to successfully capture the fuel decomposition and the formation of different products, ranging from small hydrocarbons up to four ring PAHs. The chemical pathways active during styrene pyrolysis are presented based on experimental findings and modeling assessments. Styrene consumption immediately leads to the formation of mono-aromatic hydrocarbons (benzene, phenylacetylene and o-benzyne). These aromatics then interact with other intermediates in the reaction system, resulting in the appearance of toluene, indene, naphthalene, and pyrene. Furthermore, phenyl was recognized as a significant styrene by-product. As a result, phenyl either interacts with styrene, resulting in several $C_{14}H_{12}$ PAH isomers that decompose into $C_{14}H_{10}$ isomers while releasing H-atoms, or reacts with another phenyl radical, resulting in biphenyl, which serves as an important intermediate leading to acenaphthylene via hydrogen loss and ring closure.

1 Introduction

In order to mitigate present environmental problems like air pollution, comprehensive chemical kinetic models describing polycyclic aromatic hydrocarbon (PAH) chemistry are becoming increasingly important for the development of cleaner combustion technologies. However, clarifying the complex reaction network in combustion systems remains a challenge. The discovery in recent research [1,2] that fuel pyrolysis and oxidation of resultant products are independent processes has the potential to decouple the kinetic complexity. Styrene is a prominent product with high concentration levels in the combustion and pyrolysis of aromatic compounds present in practical or surrogate fuels, such as alkylbenzenes and xylenes, and it plays a key role in the formation of PAHs. As a result, a full understanding of the chemistry involved in PAH production during styrene pyrolysis is essential and required.

The literature on gas-phase pyrolysis of styrene is relatively scarce and appears to be restricted to only three works. Sikes et al. [3] investigated the thermal decomposition of styrene in a combination of

Correspondence to: andrea.comandini@cnrs-orleans.fr

experimental, theoretical and modeling study, with a focus placed on the initial dissociation reactions. Müller-Markgraf and Troe [4] and Grela et al. [5] studied styrene pyrolysis in a shock tube (~5.5 atm, 2015 K) and a low-pressure flow reactor (~10 mTorr, 1130-1380 K), respectively, and postulated that styrene decomposes into benzene and acetylene. However, no experimental or kinetic speciation investigations on styrene pyrolysis have been published, particularly with regard to the formation of PAH compounds. Thus, the purpose of this work is to provide reliable speciation datasets utilizing shock tube and gas chromatographic (GC) techniques, as well as to update the styrene sub-mechanism in our on-going kinetic model for PAH chemistry [6]. Kinetic insights revealing the aromatic species formation from styrene pyrolysis will be presented using a combination of experimental data and modeling analyses.

2 Experimental Set-up

Styrene pyrolysis experiments are carried out with the high-purity single-pulse shock tube facility at ICARE, Orléans. Prior publications provide a thorough explanation of the experimental setup and the methodology ([6] and previous works). Briefly, the driven segment (length: 6 m; inner diameter: 78 mm) and the driver section (length: 3.7 m; inner diameter: 120 mm) of the single-pulse shock tube device are separated by a double diaphragm. The shock tube operates in a single pulse fashion as equipped with a dump tank (volume 150 L) situated close to the diaphragm section. The driven section is heated to 90 °C to prevent heavy species condensation or absorption, and it is pumped down to less than 10^{-5} mbar before each experiment. The driven section's inner surface is cleaned regularly to remove carbon deposits.

Four pressure sensors (CHIMIE METAL A25L05B) mounted on the sidewall of the driven section's end part record the time of the shock wave passage for the calculation of the incident shock velocity, which is then used to determine the post-shock conditions T_5 and P_5 by solving the conservation equations. The computed T_5 has a maximum error of 30 K due to the wave attenuation and the uncertainty in determining the exact positions of the pressure sensor sensitive surfaces [7]. A PCB Piezotronics pressure sensor located at the end-wall of the driven section measures the pressure–time profiles. The pressure profile defines the reaction time for each experiment as the time interval between the arrival of the shock wave and the point at which the pressure drops to 80% of P_5. The reaction time is around 4 ms in the current experimental configuration. The post-shock gas products behind the reflected shock waves are sampled with an air-actuated valve and are analyzed using an Agilent 7890B gas chromatograph (GC) and a Thermo Trace GC/DSQ mass spectrometer. The Agilent GC, specifically designed to measure the PAHs up to four rings, is equipped with a flame ionization detector (FID) coupled to a DB-17ms column for heavy species separation, and a thermal conductivity detector coupled to a Molseive 5A column for monitoring air absence and measurement of inert compounds. The Thermo Trace GC is equipped with an FID detector, connected to an HP Plot Q column for measuring light species up to mono-aromatics. A DSQ mass spectrometer connected to the Thermo GC aids in species identification, however, small species, MAHs and PAHs are mainly identified according to their retention time that is known from prior injection of standards. Species quantification requires calibration of the FID responses. The detectors are calibrated using standard-mixtures and gas-phase mixtures with known compositions [7]. The uncertainties in the species mole fractions are 5% for the small species and 10%-15% for the experimentally calibrated PAHs. Measurement errors for PAHs lacking experimental calibration factors may reach 20-50% or more.

In this study, shock tube pyrolysis tests were conducted at a nominal P_5 of 20 bar and a temperature range of 1160–1730 K using an argon diluted mixture containing 92 ppm styrene. The employed chemicals were styrene (98%) from Sigma-Aldrich and gas reagents such as bath gas argon (>99.9999%) and driving gas helium (> 99.995%) from Air Liquide. The mixture was prepared in a 136 L electropolished stainless steel cylinder and stayed overnight to homogenize before being used for the experiments.

3 Kinetic Modeling

The kinetic model proposed in this study aims to accurately reproduce styrene decomposition and the formation of PAH compounds under shock tube pyrolysis conditions. These efforts are a continuation of our previous serial works (latest version has been published in [6]) towards constructing a predictive kinetic model describing PAH speciation in combustion/pyrolysis of practical fuels and fuel mixtures.

The initiation decomposition steps of styrene ($C_6H_5C_2H_3$) including the ring C-H bond fission, the C-H bond fission of vinyl moiety, and the C-C bond fission are updated from the recent work of Sikes et al. [3]. The recombination reaction of o-benzyne + ethylene (C_2H_4) producing styrene is added from the LLNL PAH model reported by Shao et al. [8]. The unimolecular decomposition reaction $C_6H_5C_2H_3$=phenylacetylene($C_6H_5C_2H$)+H_2 is stated analogously to ethylbenzene($C_6H_5C_2H_5$)= $C_6H_5C_2H_3$+H_2 with activation energy multiplied by 1.13 to account for the difference in dissociation bonding energy.

Following the formation of H atoms, bimolecular reactions involving styrene/styryl radicals and H atoms occur in the reaction system. The current model structure incorporates a number of reactions from Chu et al. [9] and Sikes et al. [3] that can lead to a variety of products. In addition, the kinetic rates of the ipso-substitution reaction $C_6H_5C_2H_3$+H=C_6H_6+C_2H_3 are taken from Fahr and Stein work [10]. All of the foregoing bimolecular processes deplete the chain carrier H atoms while creating less reactive radicals. The rapid breakdown of styrene, on the other hand, shows the presence of chain-branching activities that increase the reactivity of the reaction system. In view of the abundant C_6H_5/C_2H_3/styryl radicals resulting from initiation reactions, reactions between styrene and C_6H_5/C_2H_3/styryl radicals were included in the model. Besides abstracting a hydrogen atom from styrene, C_6H_5 can add to the double carbon-to-carbon bond at the α or β site, producing two types of $C_{14}H_{13}$ adducts, $C_6H_5CH(\dot{C}H_2)C_6H_5$ and $C_6H_5\dot{C}HCH_2C_6H_5$ ($C_6H_5C_2H_3C_6H_5$), respectively. $C_6H_5\dot{C}HCH_2C_6H_5$ can decompose to stilbene ($C_6H_5C_2H_2C_6H_5$) while releasing an H atom via direct β-scission, or it can undergo intramolecular hydrogen transfer and cyclization steps leading to dihydrophenanthrene ($C_{14}H_{12}$)+H. The fate of $C_6H_5\dot{C}HCH_2C_6H_5$ was theoretically explored by Sinha and Raj [11]. Apart from the dissociation channels, chemically activated reactions: $C_6H_5C_2H_3$+C_6H_5= $C_6H_5C_2H_2C_6H_5$/$C_{14}H_{12}$+H are also added in analogy to $C_6H_5C_2H$+C_6H_5= diphenylacetylene ($C_6H_5CCC_6H_5$)/phenanthrene ($C_{14}H_{10}$)+H [12]. The C_6H_5 addition occurring at the α site and the subsequent reactions were not investigated previously to the best of our knowledge. The resulting adduct $C_6H_5CH(\dot{C}H_2)C_6H_5$ can either decompose to 1,1-diphenyl-ethylene ($C_6H_5C(CH_2)C_6H_5$) or go through intramolecular hydrogen transfer and ring closure steps, leading to 9-methyl-9H-fluorene ($C_{13}H_9CH_3$)+H. Similar to the above-mentioned reaction sequences responsible for $C_6H_5C_2H_2C_6H_5$ and $C_{14}H_{12}$ formation, stepwise conversion and a chemically activated reaction are both considered for the formation of $C_6H_5C(CH_2)C_6H_5$ and $C_{13}H_9CH_3$ in the current model. The reaction sequence rate coefficients for $C_{13}H_9CH_3$ are analogous to those for 9-methylene fluorene [12].

Both the addition/elimination reaction of benzene(C_6H_6)+C_6H_5 and the recombination reaction C_6H_5+C_6H_5 producing biphenyl ($C_6H_5C_6H_5$)+H and $C_6H_5C_6H_5$, respectively, were found to be of kinetic importance in benzene pyrolysis. Such reaction can also take place between $C_6H_5C_2H_3$/$C_6H_4C_2H_3$ and C_6H_5 or $C_6H_4C_2H_3$, producing divinyl-biphenyl ($C_2H_3C_6H_4C_6H_4C_2H_3$) compounds or vinyl-biphenyl ($C_{12}H_9C_2H_3$), respectively. The rate constants for C_6H_6+C_6H_5 = $C_6H_5C_6H_5$+H and C_6H_6+C_6H_5 = $C_6H_5C_6H_5$ are adopted for both reactions from the current kinetic model. In the current model, both $C_{12}H_9C_2H_3$ and $C_2H_3C_6H_4C_6H_4C_2H_3$ are lumped species of isomers characterized by different positions of the vinyl branches for simplification purpose.

The $C_6H_5C_2H_3$+styryl radicals ($C_6H_4C_2H_3$, C_6H_5CHCH, $C_6H_5CCH_2$) reactions can also yield to different $C_{16}H_{14}$ PAH species while directly releasing H atoms. The reaction of $C_6H_5C_2H_3$ with $C_6H_4C_2H_3$ or C_6H_5CHCH can lead to the formation of vinyl stilbene ($C_{14}H_{11}C_2H_3$). The rate coefficients for $C_6H_5C_2H_3$+$C_6H_4C_2H_3$ and $C_6H_5C_2H_3$+C_6H_4CHCH are determined through an analogy to

$C_6H_5+C_2H_4=C_6H_5C_2H_3+H$ [13] and $C_6H_6+C_2H_3=>C_6H_5C_2H_3+H$ [14], respectively. The reaction of $C_6H_5C_2H_3$ with C_6H_5CHCH can also produce 1,4-diphenyl-1,3-butadiene ($C_6H_5C_4H_4C_6H_5$). The rate coefficients for $C_6H_5C_2H_3+C_6H_4CHCH$ are assigned as that of $C_2H_4+C_2H_3=1,3C_4H_6+H$ [15]. The interactions between $C_6H_5C_2H_3$ with $C_6H_5CCH_2$ or C_6H_5CHCH can form 2,4-diphenyl-1,3-butadiene. Both reactions employ the rate constants for $C_2H_4+C_2H_3=1,3C_4H_6+H$ [15], as well as $C_6H_5C_2H_3+C_6H_5CCH_2$ leading to 2,3-diphenyl-1,3-butadiene. The reaction of $C_6H_5C_2H_3$ with $C_6H_4C_2H_3$ or $C_6H_5CCH_2$ can result in 1-phenyl-1-styryl-ethylene. The rate constants of $C_6H_5+C_2H_4=C_6H_5C_2H_3+H$ and $C_6H_6+C_2H_3=>C_6H_5C_2H_3+H$ are used for each reaction, respectively.

For the species introduced by reactions added or updated, their thermochemical data originate from the corresponding work. For those absent from literature sources, the program THERM [16] is used to compute and fit the thermochemical parameters. To simulate the experimental results, the homogenous reactor model of software COSILAB [17] is used.

4 Results and discussion

Figure 1 depicts the mole fraction profiles of the fuel and the selected intermediates as a function of T_5, incorporating measurements and simulations using two different kinetic models. The current model (red lines) can satisfactorily reproduce the fuel reactivity and speciation profiles. Integrated rate-of-production (ROP) analyses are performed at 1450 K to gain insight into the complicated chemistry inside the reaction system, when nearly half of the fuel is consumed and significant concentrations of the shown PAH compounds are present. Styrene is decomposes through reactions with H atoms, which produce 1-phenylethyl ($C_6H_5CHCH_3$), 2-phenylethyl ($C_6H_5CH_2CH_2$), and $C_6H_6+C_2H_3$. Each reaction's equivalent percentage contribution, which adds up to a total of 71%, is 11%, 27% and 33%, respectively. The rest of styrene is almost completely consumed by the unimolecular decomposition reactions (R1) $C_6H_5C_2H_3$=o-benzyne (o-C_6H_4)+C_2H_4 and (R2) $C_6H_5C_2H_3=C_6H_5C_2H+H_2$ (14% each). It is worth noting that the H-atom is consumed in favor of styrene breakdown; nevertheless, the thermal decomposition of 2-phenylethyl radical produces C_6H_5, which then attacks $C_6H_5C_2H_3$ and releases H atoms via both stepwise and direct paths. Several $C_{14}H_{12}$ compounds are formed during these processes, including stilbene (Figure 1,j) and 1,1-diphenyl-ethylene (not shown), which decompose to $C_6H_5CCHC_6H_5$ radical and 9-methylene fluorene ($C_{13}H_8CH_2$), the principal pathways leading to phenanthrene ($C_{14}H_{10}$) production (Figure 1,i). C_6H_5 either reacts with another phenyl radical leading to acenaphthylene formation ($C_{12}H_8$,Figure 1,h) through BENZO intermediate (50% at T_5=1450K) [18], or undergoes an H-abstraction reaction with styrene, which results in the creation of benzene, accounting for 10% of its formation, whereas 89% of benzene is formed directly from styrene decomposition (Figure 1,c). Phenylacetylene and ethylene (C_2H_4) are also direct products of styrene breakdown as evidenced by their early temperature window formation (Figure 1, b and e). 42% of C_2H_4 is formed by R1 and 54% through the unimolecular decomposition of $C_6H_5CH_2CH_2$. The majority of $C_6H_5C_2H$ is produced by R2 (64%) and the breakdown of styryl radicals (a total of 34%). The appearance of different mono-aromatics is crucial to the formation of various PAHs. o-Benzyne either interacts with benzene to form predominantly naphthalene (Figure 1,g) via the intermediate BICYCLO (60% at T_5=1450K) [18] or with methyl radical (CH_3) to produce benzyl, which then reacts with a hydrogen atom to produce toluene (C_7H_8 ,Figure 1,d). The breakdown of 9-methyl-9H-fluorene ($C_{13}H_9CH_3$), which is produced through the reaction $C_6H_5C_2H_3+C_6H_5$, entirely yields fluorenyl radical ($C_{13}H_9$)+CH_3. Similarly, phenylacetylene interacts with methyl to generate indene (70% at T_5=1450K) (Figure 1,f). Its radical $C_6H_4C_2H$ combines with styrene to produce 82% of pyrene ($C_{16}H_{10}$, Figure 1,l), whereas only 9% is produced by its interaction with the parent molecule, which is considered the main source of pyrene in phenylacetylene pyrolysis [12]. For the second $C_{16}H_{10}$ isomer, fluoranthene ($FC_{16}H_{10}$), two main pathways dominate its formation (Figure 1,k). The reaction between $C_{13}H_9$ and C_3H_3 and the unimolecular decomposition of phenyl naphthalene ($C_{10}H_7C_6H_5$) are the major sources of $FC_{16}H_{10}$. C_3H_3 is the result of the minor decomposition pathway of styrene ($C_6H_5C_2H_3=C_5H_5+C_3H_3$) and $C_{10}H_7C_6H_5$ is totally formed from the reaction of benzene with naphthyl radical ($C_{10}H_7$).

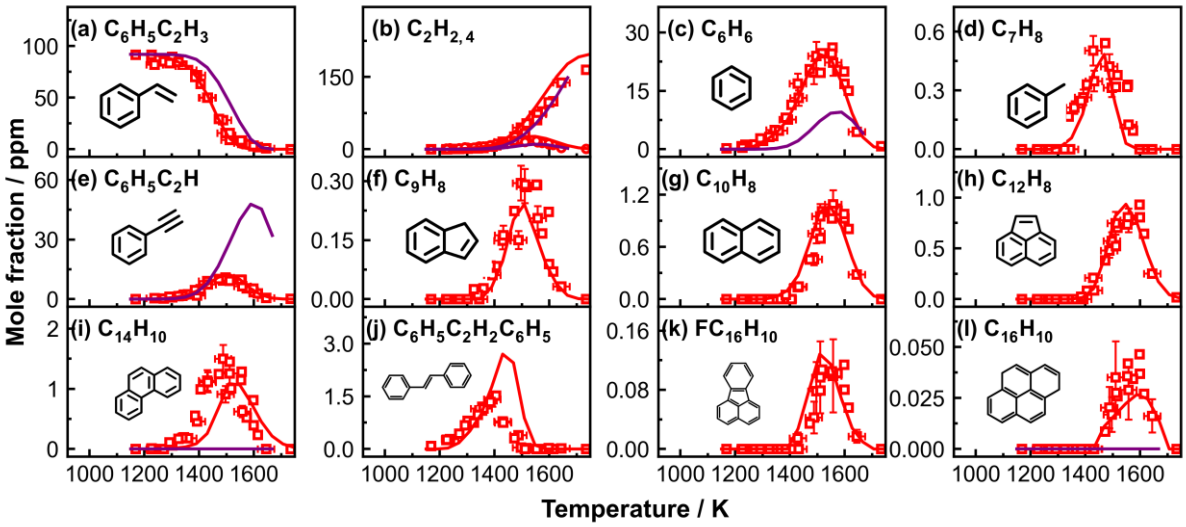

Figure 1: Measured and simulated mole fraction profiles for fuel and major products in 92 ppm styrene pyrolysis. The red solid lines are simulations using the current model. The purple solid lines are simulations using Sikes et al. [3].

5. Conclusions

This work presents a kinetic study on styrene pyrolysis based on single-pulse shock tube experiments and detailed kinetic modeling. The kinetic model can satisfactorily reproduce the measurements, regarding the fuel decomposition reactivity and the speciation of various products ranging from small molecules to up to four ring PAHs. C-H bond fission from the vinyl moiety initiates the breakdown of $C_6H_5C_2H_3$. Subsequently, the bimolecular reactions between styrene and hydrogen atoms, which results in benzene+vinyl or 2-phenylethyl, dominates styrene decomposition throughout the temperature window. Styrene decay also involves the unimolecular decomposition of styrene, which produces phenylacetylene, ethylene, and o-benzyne. The addition/elimination reactions between styrene and phenyl (primarily produced by 2-phenylethyl thermal decomposition) not only produce hydrogen atoms to maintain the reactivity of the fuel, but also directly lead to the formation of several $C_{14}H_{12}$ PAH isomers such as stilbene and 1,1-diphenyl-ethylene, which further decompose to form $C_{14}H_{10}$ PAH isomers such as $C_{13}H_8CH_2$ and $C_{14}H_{10}$. Phenyl also reacts with another phenyl radical, resulting in biphenyl, which serves as an important intermediate leading to $C_{12}H_8$ via hydrogen loss and ring closure. Benzene and phenylacetylene are significant styrene products, and their consumption leads to bigger aromatics formation. Benzene reacts either with o-benzyne leading to the formation of naphthalene or with $C_{10}H_7$ leading to the formation of $C_{10}H_7C_6H_5$, which contributes partly to $FC_{16}H_{10}$ formation. The reaction of phenylacetylene radical with styrene is the predominant pathway to $C_{16}H_{10}$.

Acknowledgment

This project has received funding from the European Research Council (ERC) under the European Union's Horizon 2020 research and innovation programme (grant agreement n° 756785).

References

[1] Malewicki T, Brezinsky K. (2013). Experimental and modeling study on the pyrolysis and oxidation of n-decane and n-dodecane. Proc. Combust. Inst.; 34:361–8.

[2] Wang H, Xu R, Wang K, Bowman CT, Hanson RK, Davidson DF, et al. (2018). A physics-based approach to modeling real-fuel combustion chemistry - I. Evidence from experiments, and thermodynamic, chemical kinetic and statistical considerations. Combust. Flame; 193:502–19.
[3] Sikes T, Banyon C, Schwind RA, Lynch PT, Comandini A, Sivaramakrishnan R, et al. (2021). Initiation reactions in the high temperature decomposition of styrene. Phys. Chem. Chem. Phys.; 23:18432–48.
[4] Mueller-Markgraf W, Troe J. (1988). Thermal decomposition of ethylbenzene, styrene, and bromophenylethane: UV absorption study in shock waves. J. Phys. Chem.; 92:4914–22.
[5] Grela MA, Amorebieta VT, Colussi AJ. (1992). Pyrolysis of styrene: kinetics and mechanism of the equilibrium styrene .tautm. benzene + acetylene. J. Phys. Chem.; 96:9861–5.
[6] Hamadi A, Piton LC, Abid S, Chaumeix N, Comandini A. (2022). Combined high-pressure experimental and kinetic modeling study of cyclopentene pyrolysis and its reactions with acetylene. Proc. Combust. Inst.
[7] Sun W, Hamadi A, Ardila FEC, Abid S, Chaumeix N, Comandini A. (2022). Insights into pyrolysis kinetics of xylene isomers behind reflected shock waves. Combust. Flame; 112247.
[8] Shao C, Kukkadapu G, Wagnon SW, Pitz WJ, Sarathy SM. (2020). PAH formation from jet stirred reactor pyrolysis of gasoline surrogates. Combust. Flame; 219:312–26.
[9] Chu T-C, Buras ZJ, Eyob B, Smith MC, Liu M, Green WH. (2020). Direct Kinetics and Product Measurement of Phenyl Radical + Ethylene. J. Phys. Chem. A; 124:2352–65.
[10] Fahr A, Stein SE. (1989). Reactions of vinyl and phenyl radicals with ethyne, ethene and benzene. Symp. (Int.) Combust.; 22:1023–9.
[11] Sinha S, Raj A. (2016). Polycyclic aromatic hydrocarbon (PAH) formation from benzyl radicals: a reaction kinetics study. Phys. Chem. Chem. Phys.; 18:8120–31.
[12] Sun W, Hamadi A, Abid S, Chaumeix N, Comandini A. (2020). An experimental and kinetic modeling study of phenylacetylene decomposition and the reactions with acetylene/ethylene under shock tube pyrolysis conditions. Combust. Flame; 220:257–71.
[13] Belisario-Lara D, Mebel AM, Kaiser RI. (2018). Computational Study on the Unimolecular Decomposition of JP-8 Jet Fuel Surrogates III: Butylbenzene Isomers (n-, s-, and t-C14H10). J. Phys. Chem. A.;122:3980–4001.
[14] Yuan W, Li Y, Dagaut P, Yang J, Qi F. (2015). Experimental and kinetic modeling study of styrene combustion. Combust. Flame; 162:1868–1883.
[15] Huang C, Yang B, Zhang F. (2017). Pressure-dependent kinetics on the C4H7 potential energy surface and its effect on combustion model predictions. Combust. Flame;181:100–9.
[16] Ritter ER, Bozzelli JW. (1991). THERM: Thermodynamic property estimation for gas phase radicals and molecules. Int. J. Chem. Kinet.;23:767–78.
[17] COSILAB, The combustion simulation laboratory, Rotexo GmbH & Co., KG, Haan, Germany, 2009 Version 3.3.2 n.d.
[18] Comandini A, Malewicki T, Brezinsky K. (2012). Chemistry of Polycyclic Aromatic Hydrocarbons Formation from Phenyl Radical Pyrolysis and Reaction of Phenyl and Acetylene. J. Phys. Chem. A.;116:2409–34.